SnO_2-decorated Multiwalled Carbon Nanotubes and Vulcan Carbon through a Sonochemical Approach for Supercapacitor Applications

Victor Vinoth, Jerry J. Wu, Abdullah M. Asiri, Teresa Lana-Villarreal, Pedro Bonete, Sambandam Anandan

PII: S1350-4177(15)30035-3
DOI: http://dx.doi.org/10.1016/j.ultsonch.2015.09.013
Reference: ULTSON 2997

To appear in: *Ultrasonics Sonochemistry*

Received Date: 29 June 2015
Revised Date: 21 September 2015
Accepted Date: 21 September 2015

Please cite this article as: V. Vinoth, J.J. Wu, A.M. Asiri, T. Lana-Villarreal, P. Bonete, S. Anandan, SnO_2-decorated Multiwalled Carbon Nanotubes and Vulcan Carbon through a Sonochemical Approach for Supercapacitor Applications, *Ultrasonics Sonochemistry* (2015), doi: http://dx.doi.org/10.1016/j.ultsonch.2015.09.013

SnO_2-decorated Multiwalled Carbon Nanotubes and Vulcan Carbon through a Sonochemical Approach for Supercapacitor Applications

Victor Vinoth[a], Jerry J. Wu[b,*], Abdullah M. Asiri[c], Teresa Lana-Villarreal[d], Pedro Bonete[d], Sambandam Anandan[a,b,*]

[a]Nanomaterials and Solar Energy Conversion Lab, Department of Chemistry, National Institute of Technology,Tiruchirappalli-620 015, India.

[b]Department of Environmental Engineering and Science, Feng Chia University Taichung-407, Taiwan.

[c]The Center of Excellence for Advanced Materials Research, King Abdulaziz University, Jeddah 21413, P.O. Box 80203, Saudi Arabia.

[d]Institut Universitari d'Electroquímica i Departament de Química Física, Universitat d'Alacant, Apartat 99. E-03080 Alacant, Spain.

[*] To whom correspondence should be addressed: E-mail: sanand@nitt.edu, jjwu@fcu.edu.tw; Tel.: +91- 431-2503639, +886-4-24517250 #5206; Fax: +91-431-2500133.312, +886-4-24517686.

Abstract

Multiwalled carbon nanotubes (MWCNTs) and Vulcan carbon **(**VC) decorated with SnO_2 nanoparticles were synthesized using a facile and versatile sonochemical procedure. The as-prepared nanocomposites were characterized by means of transmission electron microscopy, X-

ray diffraction, X-ray photoelectron spectroscopy, and Fourier transform infra red spectroscopy. It was evidenced that SnO_2 nanoparticles were uniformly distributed on both carbon surfaces, tightly decorating the MWCNTs and VC. The electrochemical performance of the nanocomposites was evaluated by cyclic voltammetry and galvanostatic charge/discharge cycling. The as-synthesized SnO_2/MWCNTs nanocomposites show a higher capacity than the SnO_2/VC nanocomposites. Concretely, the SnO_2/MWCNTs electrodes exhibit a specific capacitance of 133.33 Fg^{-1}, whereas SnO_2/VC electrodes exhibit a specific capacitance of 112.14 Fg^{-1} measured at 0.5 $mAcm^{-2}$ in 1 M Na_2SO_4.

KEYWORDS: MWCNTs; SnO_2 nanoparticles; Vulcan carbon; Ultrasound; Supercapacitor; Specific capacitance

1. INTRODUCTION

One of the challenges for the current research community is to find low-cost and environmentally friendly high-power energy resources. The electrical double layer allows for significant charge storage in the case of high-surface-area materials in contact with an electrolyte, leading to the so-called supercapacitors, electrochemical capacitors, or ultracapacitors.[1,2] Supercapacitors have been recognized as an electrical energy storage device with high power density, fast charge-discharge, and long cycle life as compared to batteries. [3,4] Supercapacitors have been significantly figured out by their increasing applications in large industrial equipments, renewable energy power plants, hybrid electric vehicles, and memory back-up devices.[5,6] Three main classes of supercapacitor materials have been described in the literatures, including metal oxide, electronically conducting polymer, and carbon-based

supercapacitors.[7-9] Recently, hybrid supercapacitors have been developed, where an activated carbon electrode was modified with a pseudo-faradaic material by increasing the capacity.[10] Of which the most extensively used carbon electrode materials is Vulcan XC-72 due to its high surface area of 250 m^2g^{-1}. [11,12] In continuation, carbon nanotubes (CNTs) have attracted research interests as supercapacitor electrode materials and have been extensively studied since their discovery in 1991. [13] In addition, CNTs have also attracted much attention due to their potentially useful structural, optical, mechanical, and electrical properties. CNTs have a novel one-dimensional tubular structure, a narrow distribution of size in the nanometer range with a highly accessible surface area, low resistivity, and high stability.[14-16] Owing to their potentiality, they have been applied in many applications, including ultrahigh-strength fibers, nanodevices, sensors, and catalyst supports.[17-19] CNTs have also been explored as candidate electrode materials for energy storage and conversion devices due to their unique structure and morphology.[20-22] Recent advances have led to the development of versatile chemical modifications, targeting CNT derivatives with even more striking features. A wide range of these derivatives have been prepared and fully characterized by exhibiting promising properties for energy conversion/storage devices, catalysis, and even for electronic nanodevices.[23-25]

On the other hand, nanoscale materials, specifically metal or metal oxide nanoparticles, are a new class of materials with interesting optical, magnetic, electronic and electrical properties.[26,27] They have unique physicochemical properties different from their corresponding bulk materials.[28,29] In the context of charge accumulation, various transition-metal oxides have shown to be excellent active materials as electrodes due to their chemical stability and variable valence.[30] Tin (IV) oxide (SnO_2) is an n-type semiconductor with a wide band gap of 3.6 eV and it has unique properties, such as optical transparency, high electrical

conductivity, high theoretical capacity (calculated to be 782 mAh g^{-1}), and low cost.[31,32] The combination of CNT and SnO_2 may lead to a new hybrid material characterized by the features of both components.[33] In fact, functional hybrid nanocomposites materials are usually formed by the combination of two or more materials with different properties, so that these components work synergistically to deliver complementary characteristics to the new material.[34,35] To the best of our knowledge, there have been only a few reports about CNT/SnO_2 composites for their application in electrochemical energy storage devices, such as lithium-ion batteries and supercapacitors.[36,37]

On the other hand, ultrasound has become an important tool in chemistry because of the extreme conditions that can be achieved by leading to unique mechanisms and reaction pathways. In recent years, sonochemistry has been applied in the synthesis of functional nanoparticles and nanostructured materials. In this methodology, energy is supplied to the system by irradiation of a liquid with high intensity ultrasonic waves in order to produce regions of extreme temperature and pressure.[38,39] In fact, the sonochemical approach has allowed to generate carbon supported nanoparticles with great uniformity while conventional preparation techniques do not provide sufficient control.[40,41]

In this work, we have prepared a SnO_2/Multiwalled Carbon Nanotube (MWCNT) and a SnO_2/Vulcan Carbon (VC) composites via a sonochemical approach. Nanoscale SnO_2 particles were found to be uniformly deposited on the surface of both substrates, VC and MWCNT, and the electrochemical properties of the as-generated materials were investigated for their application as supercapacitors. The supercapacitive behavior of SnO_2/MWCNT and SnO_2/VC was evaluated in an aqueous by galvanostatic charge/discharge measurement.

2. MATERIALS AND METHODS

2.1 Chemicals

Tin Chloride ($SnCl_2$) and ethylene glycol were purchased from Sigma Aldrich. Sulfuric acid, acetone, absolute ethanol, and trichloroethylene from Merck were used as received. High pure Vulcan XC-72R carbon was used as received from Cabot Corporation, USA. Multi-walled carbon nanotubes (MWCNT) was used as received from CNT Co., Ltd, South Korea. All other chemicals used were of analytical reagent grade and used as received without further purification. All aqueous solutions were prepared with double distilled water and all glassware was thoroughly cleaned with aqua regia (3:1 HNO_3/HCl (*v/v*)) and rinsed extensively with double distilled water before use.

2.2 Sonochemical synthesis of SnO_2/carbon hybrid nanoparticles by the Polyol method

The SnO_2 nanoparticles supported on carbon nanoparticles were prepared by the polyol assisted sonochemical method. About 100 mg of anhydrous $SnCl_2$. was dissolved in 40 ml of ethylene glycol followed by the addition of 100 mg of MWCNT. The resultant solution was subsequently irradiated with a high intensity ultrasonic horn (Ti-horn, 20 kHz and 100 W/cm^2) in air atmosphere for 3 h. After irradiation the reaction mixture was centrifuged at 10,000 rpm for 10 min and the resulting black powder was thoroughly washed with absolute ethanol several times for removing unreacted substrates. Finally, the composites was dried in vacuum at 50°C for 24 h to obtain final product (SnO_2/MWCNT).[42] Likewise, SnO_2/VC composites was also prepared. For ICP-OES analysis, the stock solutions of the metals were prepared in acidic solution. A uniform weight of carbon supported nanoparticles were stirred overnight in 3 mL of concentrated hydrochloric acid and filtered. The filtrates were made up to desired volume and

were analyzed using ICP-OES.[43] The total Sn content in SnO_2 loaded carbon samples were found to be ~29 wt.%.

2.3 Characterization

The morphology and particle size were analyzed with a high resolution transmission electron microscope (HRTEM; JEOL model JEM2010). Energy dispersive X-ray (EDX) analysis was used to determine the elements present in the nanocomposites. For SnO_2/MWCNT and SnO_2/VC, Sn in SnO_2 weight-loadings were determined using Prodigy High Dispersion ICP-OES instrument. The crystal structure and phase purity of the final products were confirmed by powder X-ray diffraction patterns (XRD) recorded with a Philips XPertPro X-ray diffractometer using the Cu Kα radiation. X-ray photoelectron spectroscopy (XPS) analysis was performed using a Physical Electronics PHI 5600 XPS spectrophotometer with a monochromatic Al Kα (1486.6 eV) excitation source. The infrared spectra were recorded employing a Thermo scientific Nicolet iS5 FT-IR spectrometer.

2.4 Electrode Fabrication and Electrochemical Characterization of the as-prepared Hybrid Nanomaterials

A supercapacitor electrode was fabricated using high-purity stainless steel (SS) plates as current collectors. The plates were first polished with successive grades of emery paper, cleaned with a soap solution, washed with double distilled water, rinsed with acetone, dried and weighed. The stainless steel substrates (Surface area: 1 cm^2) were modified with slurry composed of the as-prepared hybrid nanoparticles (75 wt.%), Vulcan XC-72 carbon (VC, 20 wt.%) and

PVDF (5 wt. %) in N-methyl-2-pyrrolidone (NMP). The slurry was uniformly distributed on the surface of the SS electrodes and finally dried in vacuum at 100°C for 12 h.

Electrochemical measurements were carried out with a potentiostat/galvanostat (AUTOLAB 302 N module) in aqueous 1 M Na_2SO_4 electrolyte at room temperature. The supercapacitance studies were carried out in a standard three-electrode cell using the hybrid nanoparticles coated stainless steel plate as a working electrode, a Pt foil as a counter electrode and an Ag/AgCl as a reference electrode. The electrochemical performance was evaluated by cyclic voltammetry (CV) and galvanostatic charge–discharge within the potential range between 0.0 V and 1.0 V vs Ag/AgCl at different scan rates (20, 40, 80, 160 and 320 mVs^{-1}).

3. Results and Discussion

In this article, the sonochemical technique was used to decorate carbon nanoparticles with highly dispersed SnO_2 nanoparticles. The sonochemical technique allows to functionalize most of the carbon nanoparticles by preventing the formation of aggregates. Additionally, it also seems to induce a more homogeneous coverage allowing the deposition of a high SnO_2 nanoparticle loading without aggregation.[44] This methodology has been employed previously in the preparation of a number of metal oxides nanoparticles on different substrates.[45-47] Since EG is a better reducing agent, SnO_2/MWCNT and SnO_2/VC composites were synthesized by combining $SnCl_2$, EG, and the carbon substrate under ultrasonic irradiation in aqueous medium. [48] The oxidation of EG is a two-step reaction so that the interaction of the -OH groups with the Mn^+ ions results in the EG oxidation to 2-hydroxyethanal (HO - CH_2 – CH = O) in a two electron process and then to oxaldehyde (O = CH – CH = O) by another two-electron process.

The released electrons from these oxidation reactions result in the reduction of the M^{n+} to M^0. [49,50] A similar mechanism can be envisaged for the reduction of Sn^{2+} and as the reaction is completed in air, Sn^0 can be easily oxidized to SnO_2.

Fig. 1 and 2 show the TEM images of the sonochemically prepared composites based on MWCNT and VC modified with SnO_2 nanoparticles. Fig. 1A and 1B depict the SnO_2/MWCNT composites morphology at different scales, illustrating the absence of nanoparticle aggregates. The size of the SnO_2 nanoparticle (5-8 nm) in SnO_2/MWCNT composites and lattice fringes are clearly visible in the HRTEM image (Fig. 1C), which demonstrates the crystal nature of SnO_2 nanoparticles decorated on to the MWCNT. EDX studies detected C, O and Sn signals, confirming the SnO_2 nanoparticles decorated on the MWCNT (Fig. 1D). The main diffraction lines of SAED have been assigned to (110), (1 1 2), and (2 2 1) planes of the SnO_2 phase. (Fig. 1E). Fig. 2 shows TEM images of the as-prepared SnO_2/VC composites, which has spherical-like morphology with diameters in the range of 3-8 nm with higher degree of dispersion of the SnO_2 nanoparticles on the carbon surface (Fig. 2A and 2B). In Fig. 2C, EDX spectrum also confirms well for the formation of SnO_2/VC composites. In SAED diffraction lines, (110), (112), and (221) planes are assigned to the SnO_2 phase as shown in Fig. 2D. According to the ring patterns, it can be concluded that the powder is polycrystalline.

Fig. 3 shows the corresponding XRD patterns for (A) SnO_2/MWCNT and (B) SnO_2/VC nanocomposites. In both cases, the basic diffraction peaks of graphitic carbon were observed at $2\theta = 26°$. This can be attributed to the (002) plane of the graphitic structure (JCPDS No: 75-1621). The other diffraction peaks at 26°, 44°, 53.3°, and 78.8° can be indexed to (110), (112), (221), and (330) planes (JCPDS No:29-1484) of SnO_2, indicating the crystal structure of the as-grown SnO_2 nanoparticles on both surfaces, i.e. on MWCNT and VC. The basic broad peaks of

Vulcan Carbon XC-72 are also observed at about 26° and 44°. As observed for both the composites, the main SnO_2 diffraction peaks are superimposed on the main graphitic carbon diffraction peak. Both of SnO_2/MWCNT and SnO_2/VC possess identical XRD patterns with broad diffraction peaks, indicating the small size of the SnO_2 particles.[51]

XPS was performed for SnO_2/MWCNT nanocomposites to further confirm the chemical nature of the SnO_2 nanoparticles. The Sn 3d high-resolution spectrum recorded for the as-prepared SnO_2/MWCNT nanocomposites shows two main peaks at 486.8 eV and 495.2 eV, which are characteristic of $3d_{5/2}$ and $3d_{3/2}$ states of SnO_2 (Fig. 4A). The separation between these two peaks is about 8.4 eV, which is in good agreement with the energy splitting previously reported for SnO_2.[52,53] Fig. 4B shows the C1s high resolution spectrum at 283.6 eV, which corresponds to the energy of the C1s core level for aromatic rings and the peak at 288.6 eV corresponding to oxygen carbon (-COO) bonding.[54,55] For comparison, the as-prepared SnO_2/VC nanocomposites were also characterized by XPS (Fig. 5A and 5B), as expected the characteristics states of Sn in SnO_2 and C1s were observed in extended spectrum. Moreover, there is no peak assigned to other chemical states of Sn, confirming the formation of SnO_2 nanoparticles on the surfaces of MWCNT and VC. The binding energy of Sn and C1s had the same value in both composites. Thus, the XPS results confirm that the heterostructures are composed of SnO_2 and MWCNTs and VC.

In Fig. 6 curves (a) to (d) show FT-IR spectra for (a) VC, (b) SnO_2/VC, (c) pristine MWCNT, and (d) SnO_2/MWCNT, respectively. All the spectra are virtually identical. A band at 3438 cm^{-1} can be seen, which is attributed to the O-H stretching vibration of adsorbed water molecules and surface OH groups. A typical band at 1635 cm^{-1} is assigned to conjugated sp^2 C=C stretching and the peaks observed at 1740 cm^{-1} and 1070 cm^{-1} correspond to C=O and C-O

stretching vibrations of the carboxylic groups (–COOH). The absorption bands at 2921 and 2851 cm^{-1} can be attributed to the C-H stretching. More interestingly, in the curves (b) and (d), a new peak is noticed at 817 cm^{-1} which may be characteristic of the O–Sn–O stretching bonds.[56,57] Therefore, the FTIR analysis further confirms that SnO_2 nanoparticles are decorating on the MWCNT and the VC surfaces.[58]

SnO_2/MWCNT and SnO_2/VC electrodes were characterized by cyclic voltammetry in 1.0 M Na_2SO_4 solution using a working potential window between 0 – 1 V vs Ag/AgCl electrode and different scan rates 20, 40, 80, 160, and 320 mVs^{-1} (Fig. 7A and 7B). No apparent contribution of any pseudofaradic process was clearly observed in the cyclic Voltammograms (CVs) for both the nanocomposites. Furthermore, no obvious distortion was observed in the CVs as the potential scan rate increased. Even at a very high scan rate such as 320 mVs^{-1}, the CV still retains the rectangular shape. The outstanding CV shape at such a high scan rate reveals a very rapid response that implies not only a high electrode conductivity,[59,60] but also the electrolyte ions undergo very fast diffusion in the composites.[61] Therefore, we can expect a very low equivalent series resistance (ESR) for these electrodes in accordance with the vertical rectangular sides of the CVs.[62] For comparison, Fig. 7C shows the CVs of SnO_2/MWCNT and SnO_2/VC nanocomposites electrodes at 320 mV s^{-1}. The current of SnO_2/MWCNT electrodes is 2 times that observed for the SnO_2/VC composites electrodes. A more rectangular shape for the CVs was observed for SnO_2/MWCNT as compared with SnO_2/VC composites electrode, indicating a more ideal capacitor character.[63] The result could be related with the higher conductivity of the MWCNT compared to VC. Another possible explanation is that the final electrode nanoarchitecture of both electrodes is very different. One could expect a more open structure in the case of MWCNT that could facilitate the electrolyte access. In any case, we cannot

completely discard a different contribution/coverage of the SnO_2 nanoparticles in both composites.

The electrochemical performance was further studied using galvanostatic charge/discharge measurements. Fig. 8A shows the galvanostatic charge-discharge behavior of a SnO_2/MWCNT nanocomposites electrode with an applied constant current of 0.5 mA in the potential range between 0 and +1 V vs Ag/AgCl electrode. For SnO_2/VC (Fig. 8B (a)), the charge/discharge curve exhibits a deviation from a symmetrical triangular shape compared to SnO_2/MWCNT (Fig. 8B (b)), implying that the combination of electrical double layer (EDL) capacitance with Faradaic capacitance. The specific capacitance (SC, Fg^{-1}) of the electrodes can be calculated from the discharge time using the following equation:[64]

$$SC = it/\Delta Vm$$

where SC is the specific capacitance by mass of electroactive material, i is the current density (A), t is the discharge time in seconds, ΔV is the potential window (V), and m is the mass of the electroactive material (g). The specific capacitance values obtained in this way for MWCNT, SnO_2/VC, and SnO_2/MWCNT from the galvanostatic charge/discharge curves are 74.07 Fg^{-1}, 112.14 Fg^{-1}, and 133.33 Fg^{-1}, respectively. The capacitance value (133.33 Fg^{-1}) obtained here is comparatively higher than previous literature values (113 and 93 Fg^{-1} for SnO_2/MWCNT).[65,66] Certainly, MWCNTs can facilitate a fast electron transport maintaining an open structure with a high surface electrolyte–electrode interface that can facilitate a high capacity value.[67,68]

Conclusion

In summary, SnO_2/MWCNT and SnO_2/VC heterostructures have been synthesized by employing a sonochemical method. The XRD results, TEM images, and the corresponding EDX analysis revealed the presence of SnO_2 nanoparticles on the surface of the MWCNT and VC. Further analysis by XPS and FT-IR spectroscopy also confirmed the formation of SnO_2 nanoparticles on the carbon surface. The investigation of the electrochemical behavior showed a rectangular shape for the CVs even at high scan rates of 320 mV^{-1}, indicating that the composites, particularly SnO_2/MWCNT, are promising materials for supercapacitor electrodes. The current observed for SnO_2/MWCNT electrodes is two times increases upon compared to SnO_2/VC composites electrodes, due to stability of defective structure and improvement of charge transfer between SnO_2/MWCNT and electrolyte. The specific capacitance of 133.33 Fg^{-1} for SnO_2/MWCNT electrode from charge–discharge measurement is an indication that the as-synthesized nanocomposites is a potential candidate for supercapacitor application.

ACKNOWLEDGEMENT

SA thanks the Feng Chia University in Taiwan for the Visiting Professor appointment. The author SA and TLV thank DST, New Delhi for the sanction of India–Spain collaborative research grant (DST/INT/Spain/P-37/11 dt.16th Dec 2011) and Generalitat Valenciana for the financial support through ACOMP/2014/137. In addition, acknowledgement is also given to the financial support of Ministry of Science and Technology, Taiwan, at the grant number of NSC-101-2221-E-035-031-MY3. The support in providing the fabrication and measurement facilities from the Precision Instrument Support Center of Feng Chia University is also acknowledged

REFERENCE

[1] M. Winter, R. J. Brodd, What Are Batteries, Fuel Cells, and Supercapacitors?, Chem. Rev. 104 (2004) 4245-4269.

[2] J. R. Miller, P. Simon, Electrochemical Capacitors for Energy Management, Science 321 (2008) 651-652.

[3] C. C. Hu, K. H. Chang, C. C. Wang, Two-step hydrothermal synthesis of Ru–Sn oxide composites for electrochemical supercapacitors, Electrochim. Acta 52 (2007) 4411-4418.

[4] A. Burke, Ultracapacitors: why, how, and where is the technology, J. Power Sources 91 (2000) 37-50.

[5] A. Kuperman, I. Aharon, Battery–ultracapacitor hybrids for pulsed current loads, Renew Sust Energ Rev 15 (2011) 981-992.

[6] X. Zhao, B. M. Sanchez, P. J. Dobson, P. S. Grant, The role of nanomaterials in redox-based supercapacitors for next generation energy storage devices, Nanoscale 3 (2011) 839-855.

[7] H. Y. Lee, J. B. Goodenough, Supercapacitor Behavior with KCl Electrolyte, J. Solid State Chem. 144 (1999) 220-223.

[8] W. C. Chen, T. C. Wen, H. Teng, Polyaniline-deposited porous carbon electrode for supercapacitor, Electrochim. Acta 48 (2003) 641-649.

[9] D. L. Castello , D. C. Amoros , A. L. Solano , S. Shiraishi , H. Kurihara , A. Oya, Influence of pore structure and surface chemistry on electric double layer capacitance in non-aqueous electrolyte, Carbon 41 (2003) 1765–1775.

[10] G. H. Yuan , Z. H. Jiang, A. Aramata, Y. Z. Gao, Electrochemical behavior of activated-carbon capacitor material loaded with nickel oxide, Carbon 43 (2005) 2913–2917.

[11] S. L. Candelaria, Y. Shao, W. Zhou, X. Li, J. Xiao, J. G. Zhang, Y. Wang, J. Liu, J. Li, G. Cao, Nanostructured carbon for energy storage and conversion, Nano Energy 1 (2012) 195–220.

[12] X. Zhao, H. Tian, M. Zhu, K. Tian, J.J. Wang, F. Kang, R.A. Outlaw, Carbon nanosheets as the electrode material in supercapacitors, J. Power Sources 194 (2009) 1208–1212.

[13] S. Iijima, Helical microtubules of graphitic carbon, Nature 354 (1991) 56-58.

[14] R. Saito, G. Dresselhaus, M.S. Dresselhaus, Electronic structure of double-layer graphene tubules, J. Appl. Phys. 73 (1993) 494-500.

[15] R. Saito, M. Fujita, G. Dresselhaus, M.S. Dresselhaus , Electronic structure of chiral graphene tubules, Appl. Phys. Lett. 60 (1992), 2204-2206.

[16] T. W. Ebbesen, H. J. Lezec, H. Hiura, J. W. Bennett, H. F. Ghaemi, T. Thio, Electrical conductivity of individual carbon nanotubes, Nature 382 (1996) 54-56.

[17] A. Vijayaraghavan, K. Kanzaki, S. Suzuki, Y. Kobayashi, H. Inokawa, Y. Ono, S. Kar, P. M. Ajayan, Metal−semiconductor transition in single-walled carbon nanotubes induced by low-energy electron irradiation, Nano lett. 5 (2005) 1575-1579.

[18] S. F. Wang, L. Shen, W. D. Zhang, Y. J. Tong, Preparation and mechanical properties of chitosan/carbon nanotubes composites, Biomacromolecules 6 (2005) 3067-3072.

[19] X. Gui, J. Wei, K. Wang, A. Cao, H. Zhu, Y. Jia, Q. Shu, D. Wu, Carbon Nanotube Sponges Adv. Mater. 22 (2010) 617-621.

[20] P. Simon, Y. Gogotsi, Materials for electrochemical capacitors, Nat. Mater. 7 (2008) 845-854.

[21] E. Frackowiak, Carbon materials for supercapacitor application, Phys Chem. Chem. Phys. 9 (2007) 1774-1785.

[22] M. Noked, S. Okashy, T. Zimrin, D. Aurbach, Composite Carbon Nanotube/Carbon Electrodes for Electrical Double-Layer Super Capacitors, Angew. Chem. Int. Ed. 51 (2012) 1568-1571.

[23] R. H. Baughman, A. A. Zakhidov, W. A. de Heer, Carbon Nanotubes-the route toward applications, Science 297 (2002) 787-792.

[24] S. Banerjee, M. G. C. Kahn, S. S. Wong, Rational Chemical Strategies for Carbon Nanotube Functionalization, Chem. Eur. J. 9 (2003) 1898-1908.

[25] D. M. Guldi, G. M. A. Rahman, F. Zerbetto, M. Prato, Carbon Nanotubes in Electron Donor – Acceptor Nanocomposites, Acc. Chem. Res. 38 (2005) 871-878.

[26] D. Tasis, N. Tagmatarchis, A. Bianco, M. Prato, Chemistry of carbon nanotubes, Chem. Rev. 106 (2006) 1105-1136.

[27] C. N. R. Rao and A. K. Cheetham, Science and technology of nanomaterials: current status and future prospects J. Mater. Chem. 11 (2001) 2887-2894.

[28] P. D. Cozzoli, T. Pellegrino, L. Manna, Synthesis, properties and perspectives of hybrid nanocrystal structures, Chem. Soc. Rev. 35 (2006) 1195-1208.

[29] H. Zhang, M. Jin and Y. Xia, Enhancing the catalytic and electrocatalytic properties of Pt-based catalysts by forming bimetallic nanocrystals with Pd, Chem. Soc. Rev., 41 (2012) 8035–8049.

[30] H. You, S. Yang, B. Ding, H. Yang, Synthesis of colloidal metal and metal alloy nanoparticles for electrochemical energy applications, Chem. Soc. Rev., 42 (2013) 2880–2904.

[31] J.P. Zheng, P.J. Cygan, T.R. Jow, Hydrous ruthenium oxide as an electrode material for electrochemical capacitors, J. Electrochem. Soc. 142 (1995) 2699–2703.

[32] S.P. Lim, N.M. Huang, H.N. Lim, Solvothermal synthesis of SnO_2/graphene nanocomposites for supercapacitor application, Ceram.Int. 39 (2013) 6647-6655.

[33] X. Wang, X. Zhou, K. Yao, J. Zhang, Z. Liu, A SnO_2/graphene composite as a high stability electrode for lithium ion batteries, Carbon 49 (2011) 133-139.

[34] G. G. Wildgoose, C. E. Banks, R. G. Compton, Metal nanopartictes and related materials supported on carbon nanotubes: Methods and applications, Small 2 (2006) 182-193.

[35] H. Bai, C. Li, G.Q Shi, Functional Composite Materials Based on Chemically Converted Graphene, Adv. Mater. 23 (2011) 1089 – 1115.

[36] N. A. Kaskhedikar, J. Maier, Adv. Mater. 21 (2009) 2664 – 2680.

[37] J. Liang, W. Wei, D. Zhong, Q. Yang, L. Li, L. Guo, One-Step In situ Synthesis of SnO_2/Graphene Nanocomposites and its Application as an Anode Material for Li-Ion Batteries, ACS Appl. Mater. Interfaces 4 (2012) 454-459.

[38] F. Li, J. Song, H. Yang, S. Gan and Q. Zhang, One-step synthesis of graphene/SnO_2 nanocomposites and its application in electrochemical supercapacitors Nanotechnology, 20 (2009) 455602 (6pp).

[39] A. Gedanken, Using sonochemistry for the fabrication of nanomaterials, Ultrason. Sonochem. 11 (2004) 47–55.

[40] J.H. Bang, K. Suslick, Applications of Ultrasound to the Synthesis of Nanostructured Materials, Adv. Mater. 22 (2010) 1039-1059.

[41] K. Okitsu, A. Yue, S. Tanabe, H. Matsumoto, Sonochemical preparation and catalytic behavior of highly dispersed palladium nanoparticles on alumina, Chem. Mater. 12 (2000) 3006–3011.

[42] S. Anandan, A. M. Asiri, M. Ashokkumar, Ultrasound assisted synthesis of Sn nanoparticles-stabilized reduced graphene oxide nanodiscs, Ultrason. Sonochem. 21 (2014) 920–923.

[43] M. Li, A. Kowal, K. Sasaki , N. Marinkovic, D. Su, E. Korach, P. Liu, R. R. Adzic, Ethanol oxidation on the ternary Pt–Rh–SnO_2/C electrocatalysts with varied Pt:Rh:Sn ratios, Electrochim. Acta 55 (2010) 4331–4338.

[44] T. Fujimoto, S. Teraushi, H. Umehara, I. Kojima, W. Henderson, Sonochemical preparation of single-dispersion metal nanoparticles from metal salts, Chem. Mater. 13 (2001) 1057–1060.

[45] Y. Xing, Synthesis and electrochemical characterization of uniformly-dispersed high loading Pt nanoparticles on sonochemically-treated carbon nanotubes, J. Phys. Chem. B. 108 (2004) 19255 – 19259.

[46] J. M. Campelo, D. Luna, R. Luque, J. M. Marinas, A. A. Romero, Sustainable Preparation of supported metal nanoparticles and their applications in catalysis, ChemSusChem 2 (2009) 18 - 45.

[47] R. V. Kumar, Y. Diamant, A. Gedanken, Sonochemical synthesis and characterization of nanometer-size transition metal oxides from metal acetates, Chem. Mater. 12 (2000) 2301 - 2305.

[48] L. Qiu, V. G. Pol, J. C. Moreno, A. Gedanken, Synthesis of tin nanorods via a sonochemical method combined with a polyol process, Ultrasonic. Sonochem. 12 (2005) 243–247.

[49] C. Bock, C. Paquet, M. Couillard, G. A. Botton, B. R. MacDougall, Size-Selected Synthesis of PtRu Nano-Catalysts: Reaction and Size Control Mechanism, J. AM. CHEM. SOC. 126 (2004) 8028 – 8037.

[50] R. J. Joseyphus, T. Matsumoto, H. Takahashi, D. Kodama, K. Tohji, B. Jeyadevan, Designed synthesis of cobalt and its alloys by polyol process, J. Solid State Chem.180 (2007) 3008–3018.

[51] J. Zhu, Z. Lu, S. T. Aruna, D. Aurbach, A. Gedanken, Sonochemical synthesis of SnO_2 nanoparticles and their preliminary study as Li insertion electrodes, Chem. Mater. 12 (2000) 2557 - 2566.

[52] F. M. Courtel, E. A. Baranova, Y. A. Lebdeh, I. J. Davidson, In situ polyol-assisted synthesis of nano-SnO_2 /carbon composite materials as anodes for lithium-ion batteries, J. Power Sources 195 (2010) 2355–2361.

[53] B. Venugopal, B. Nandan, A. Ayyachamy, V. Balaji, S. Amirthapandian, B. K. Panigrahi, T. Paramasivam, Influences of manganese ions in the band gap of tin oxide nanoparticles: structure, microstructure and optical studies, RSC Adv. 4 (2014) 6141–6150.

[54] J. G. Kim, S. H. Lee, S. H. Nam, S. M. Choi, W. B. Kim, Standing pillar arrays of C-coated hollow SnO_2 mesoscale tubules for a highly stable lithium ion storage electrode, RSC Adv. 2(2012) 7829–7836.

[55] Y. Liu, X. Jing, Pyrolysis and structure of hyperbranched polyborate modified phenolic resins, Carbon 45 (2007) 1965–197.

[56] X. Meng, Y. Zhong, Y. Sun, M. N. Banis, R. Li, X. Sun, Nitrogen-doped carbon nanotubes coated by atomic layer deposited SnO_2 with controlled morphology and phase, Carbon 49 (2011) 1133 – 1144.

[57] Y. S. Jung, K. T. Lee, J. H. Ryu, D. Im, and S. M. Oh, Sn-carbon core-shell powder for anode in lithium secondary batteries, J. Electrochem. Soc. 152 (2005) A1452–A1457.

[58] D. Hernandez, F. Mendoza, E. Febus, B. R. Weiner, G. Morell, Binder Free SnO_2-CNT Composite as Anode Material for Li-Ion Battery, J. Nanotechnology (2014) 1-9.

[59] G. Wang, L. Zhang, J. Zhang, A review of electrode materials for electrochemical supercapacitors, Chem. Soc. Rev., 41(2012) 797–828.

[60] H. Pan, J. Li, Y. P. Feng, Carbon Nanotubes for Supercapacitor, Nanoscale Res Lett., 5 (2010) 654–668.

[61] H. W. Chang, Y.R. Lu, J. L Chen, C. L. Chen, J. F. Lee, J. M. Chen, Y. C. Tsai, C. M. Chang, P. H. Yeh, W. C. Chou, Y. H. Lioug, C. L. Dong, Nanoflaky MnO_2/functionalized carbon nanotubes for supercapacitors: an in situ X-ray absorption spectroscopic investigation, Nanoscale 7 (2015) 1725-1735.

[60] H. Tong, H. L. Li, X. G. Zhang, Ultrasonic synthesis of highly dispersed Pt nanoparticles supported on MWCNTs and their electrocatalytic activity towards methanol oxidation, Carbon 45 (2007) 2424–2432.

[61] J. Yan, Z. Fan, T. Wei, J. Cheng, B. Shao, K. Wang, L. Song, M. Zhang, Carbon nanotubes/MnO_2 composites synthesized by microwave assisted method for supercapacitors with high power and energy densities, J. Power Sources 194 (2009) 1202–1207.

[62] M. D. Stoller, R. S. Ruoff, Best practice methods for determining an electrode material's performance for ultracapacitors, Energy Environ. Sci., 3 (2010) 1294–1301.

[63] K. C. Ng, S. Zhang, C. Peng, G. Z. Chen, Individual and Bipolarly Stacked Asymmetrical Aqueous Supercapacitors of CNTs/SnO_2 and CNTs/MnO_2 Nanocomposites, J. Electrochem. Soc.156 (2009) A846-A853.

[64] A. L. M. Reddy, S. Ramaprabhu, Nanocrystalline metal oxides dispersed multiwalled carbon nanotubes as supercapacitor electrodes, J. Phys. Chem. C 111 (2007) 7727 – 7734.

437 [65] W. Chen, Z. Fan, L. Gu, X. Bao, C. Wang, Enhanced capacitance of manganese
438 oxide via confinement inside carbon nanotubes, Chem. Commun. 46 (2010) 3905–3907.
439 [66] W. D. Zhang, J. Chen, Fabrication of a vertically aligned carbon nanotube
440 electrode and its modification by nanostructured MnO_2 for supercapacitors, Pure Appl.
441 Chem. 81 (2009) 2317–2325.
442
443

Figures

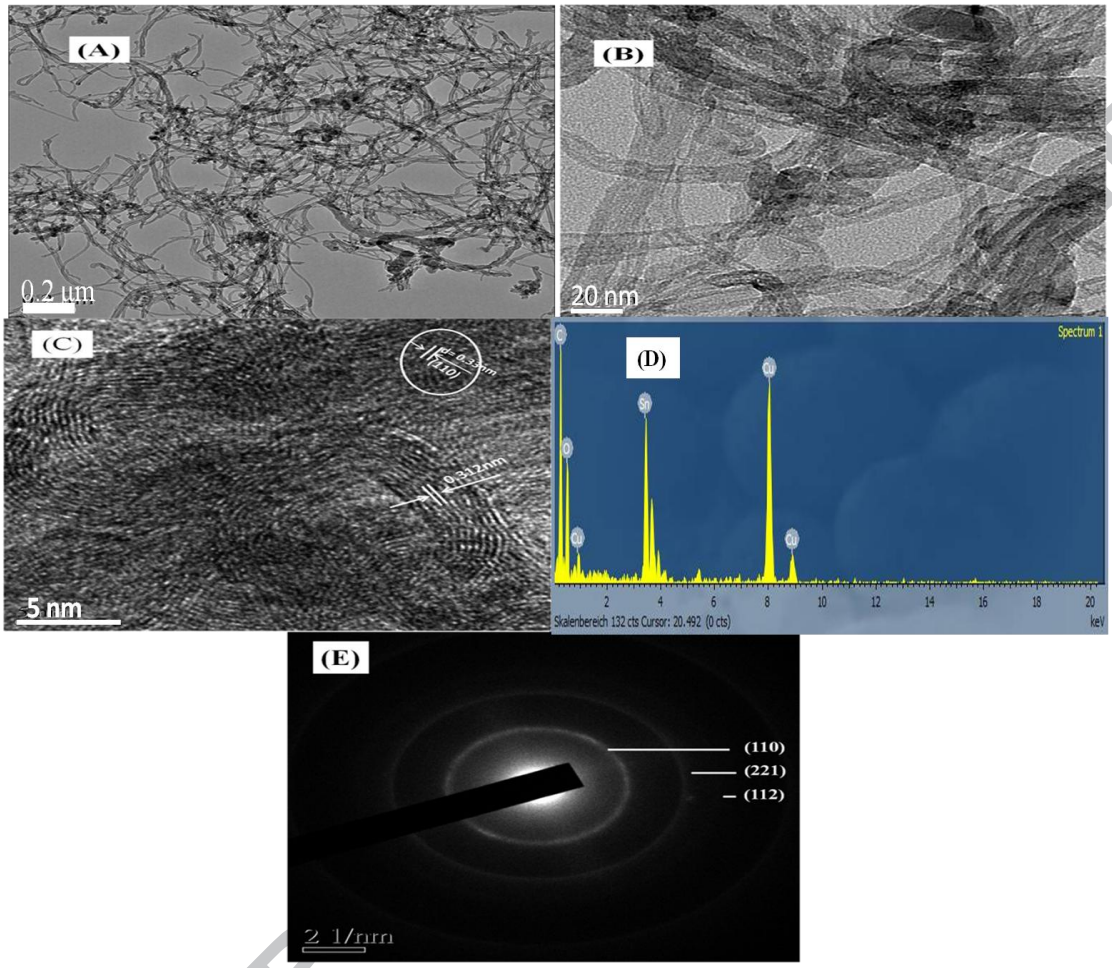

Fig. 1. TEM images of the SnO_2 /MWCNT composite (A, B and C) represent images at different scales. (D) Energy dispersive spectrum of SnO_2 /MWCNT composite. (E) SAED pattern, showing both the diffraction rings of SnO_2 nanoparticles and diffraction spots of MWCNT

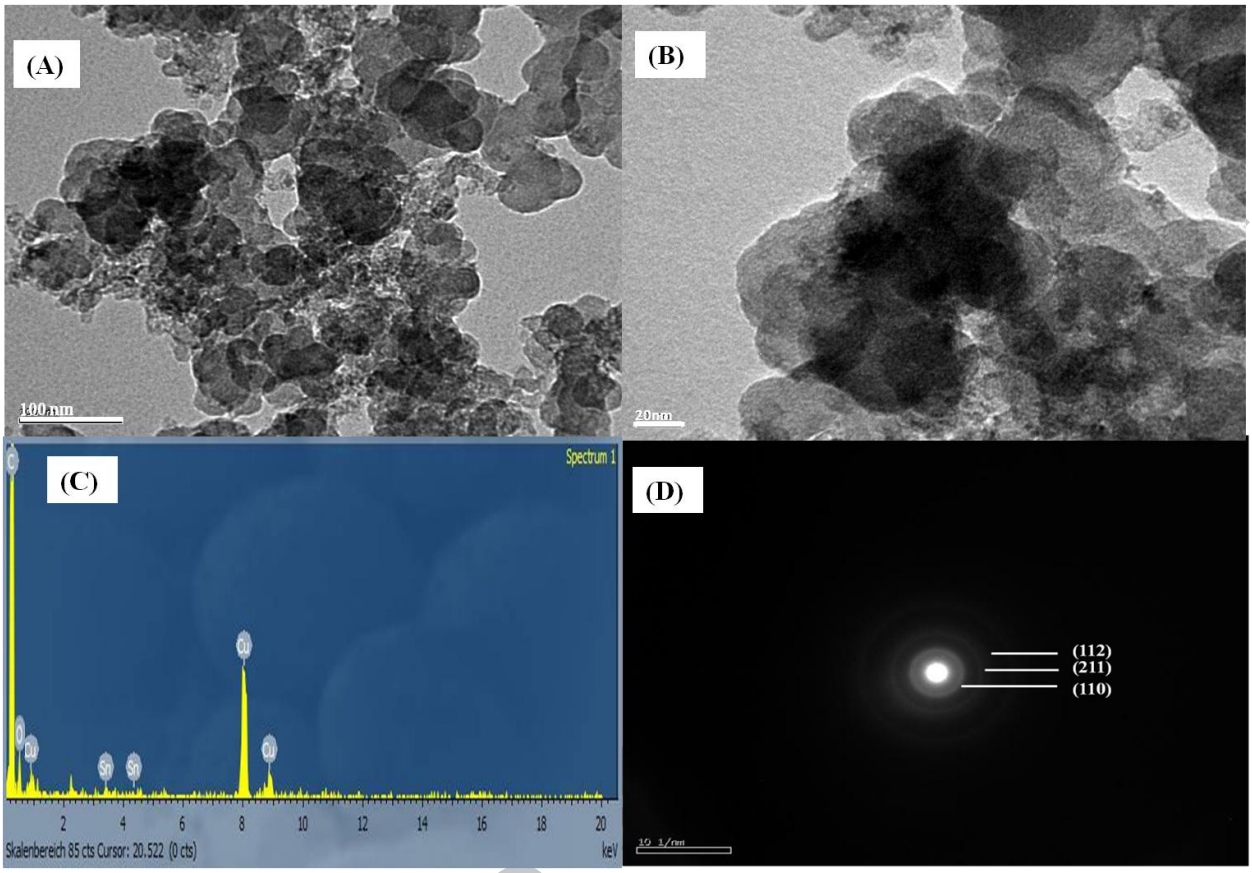

Fig. 2. TEM (A and B), EDX(C) and SAED (D) image of the SnO_2 /VC composite

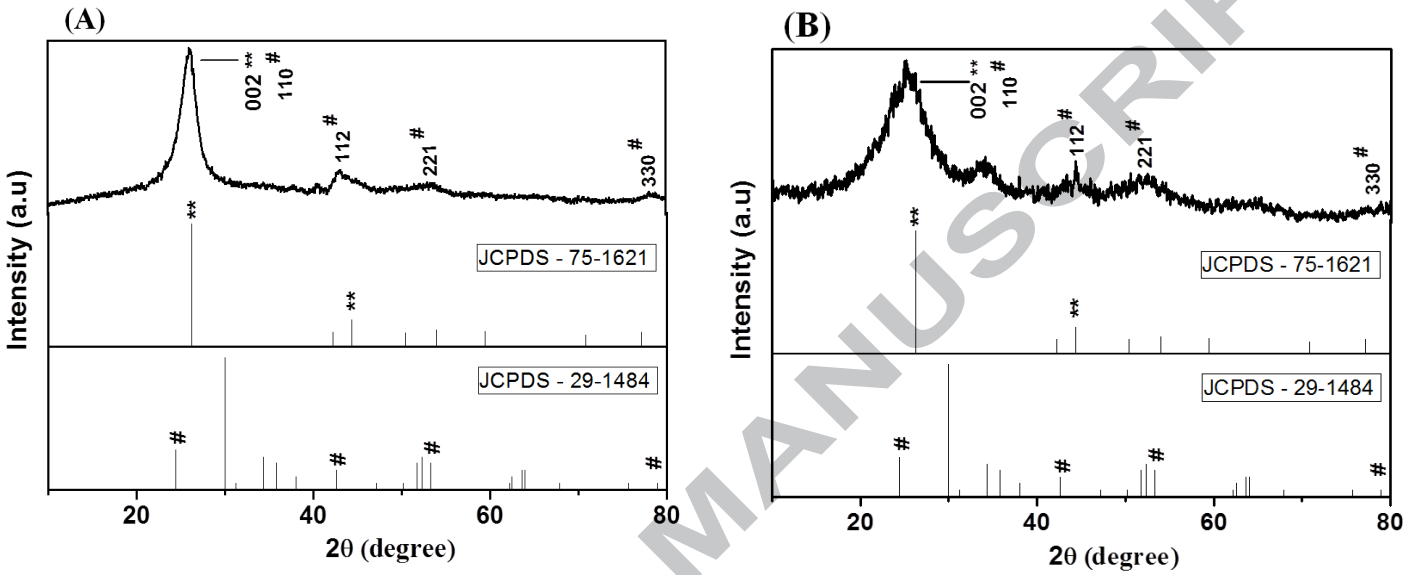

Fig. 3. XRD pattern of sonochemically prepared composites. (A) SnO_2/MWCNT composites. (B) SnO_2/VC composites

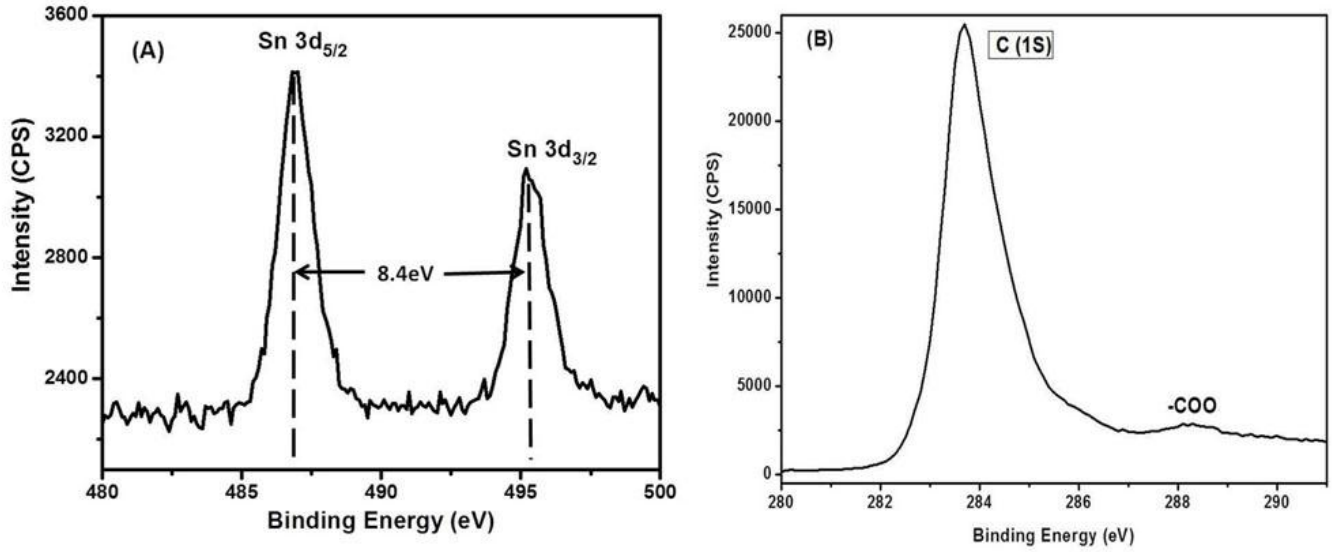

Fig. 4. X-ray photoelectron high-resolution spectrum of Sn3d (A) and the high-resolution spectra of C1s (B) for sonochemically prepared SnO_2/MWCNT composites

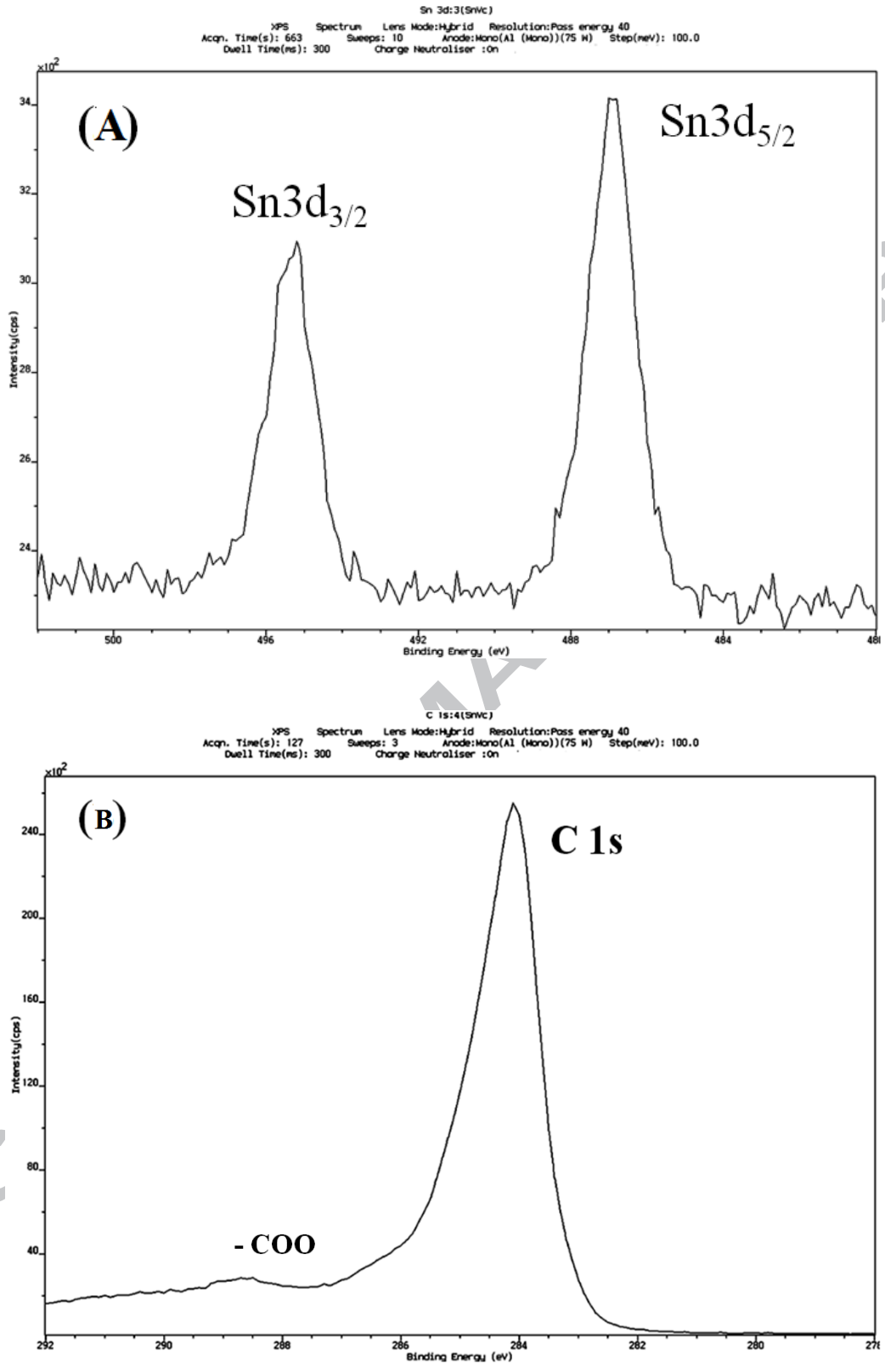

Fig. 5. X-ray photoelectron high-resolution spectrum of Sn3d (A) and the high-resolution spectra of C1s (B) for sonochemically prepared SnO_2/VC composites

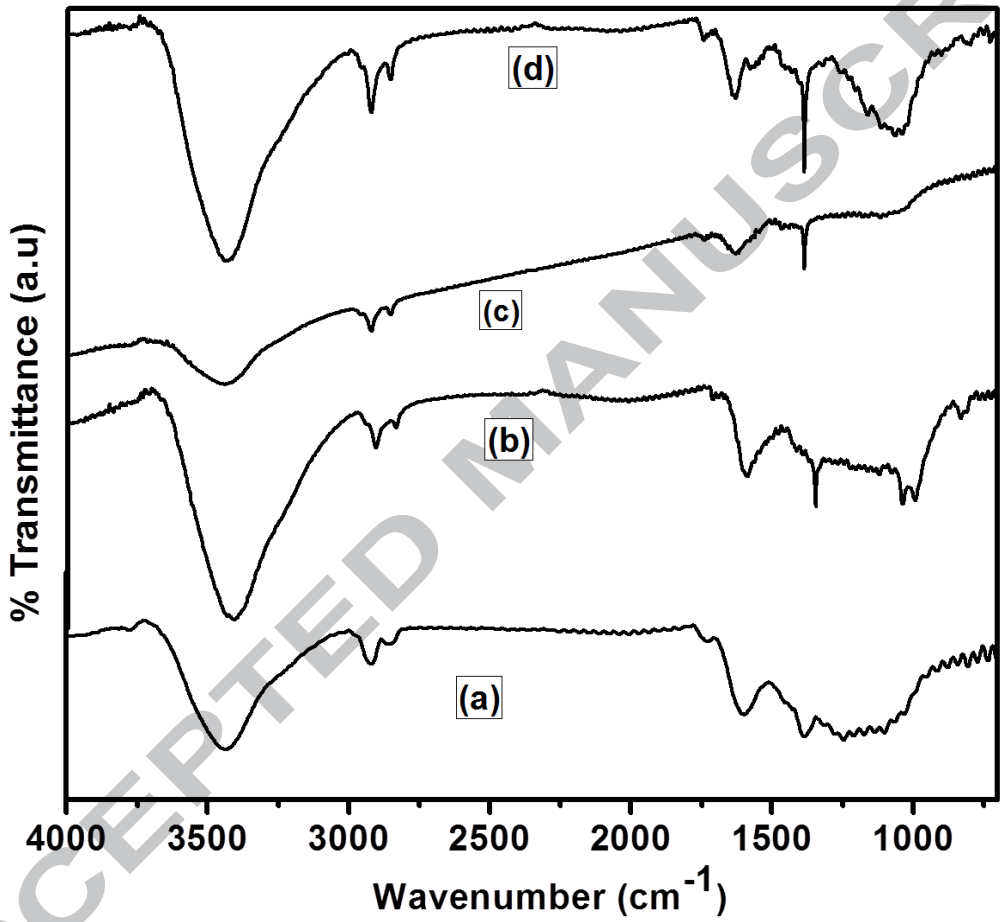

Fig. 6. Fourier transform infrared spectra of (a) VC, (b) SnO_2/VC composite(c) pristine MWCNT and (d) SnO_2/MWCNT composite.

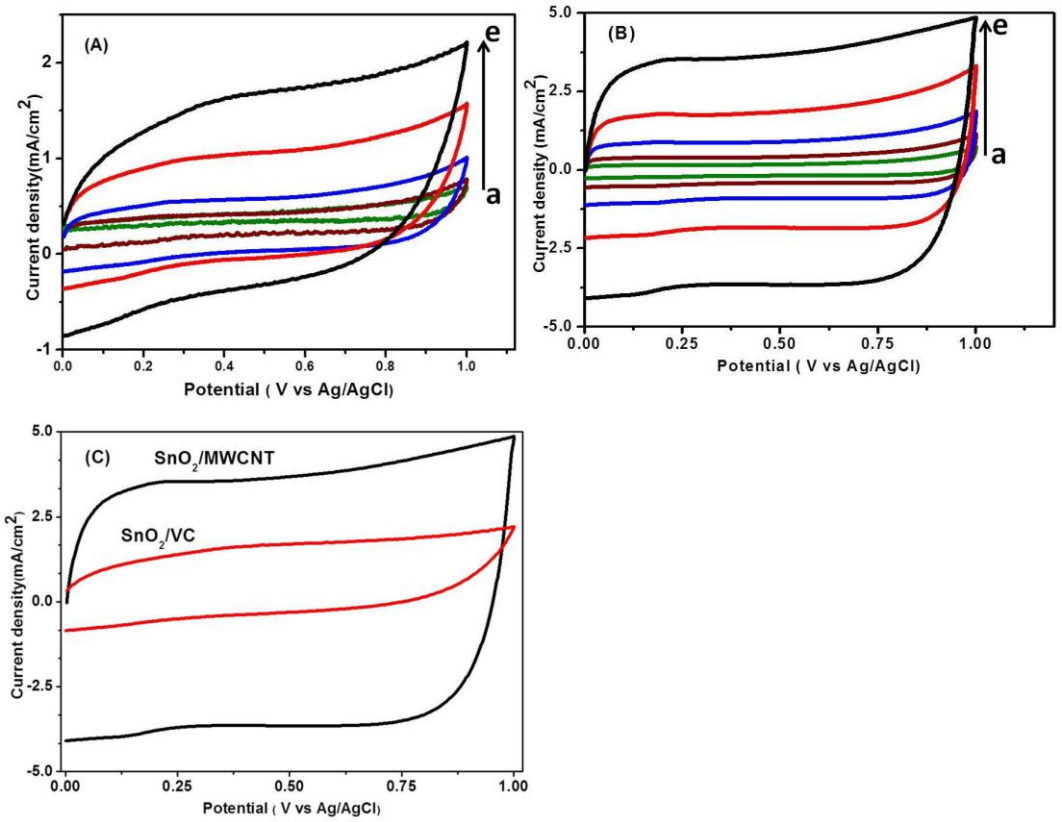

Fig. 7. Cyclic voltammogram (CVs) of SnO_2/VC composites (A) and SnO_2/MWCNT composites (B) recorded at different scan rates of 20, 40, 80, 160 and 320 mVs^{-1}(a–f) in the potential window of 0 to 1 V vs. Ag/AgCl in aqueous solution of 1M Na_2SO_4 electrolyte. (C) CVs of SnO_2/VC and SnO_2/MWCNT composites 1.0 M Na_2SO_4 at a scan rate of 320 mVs^{-1}

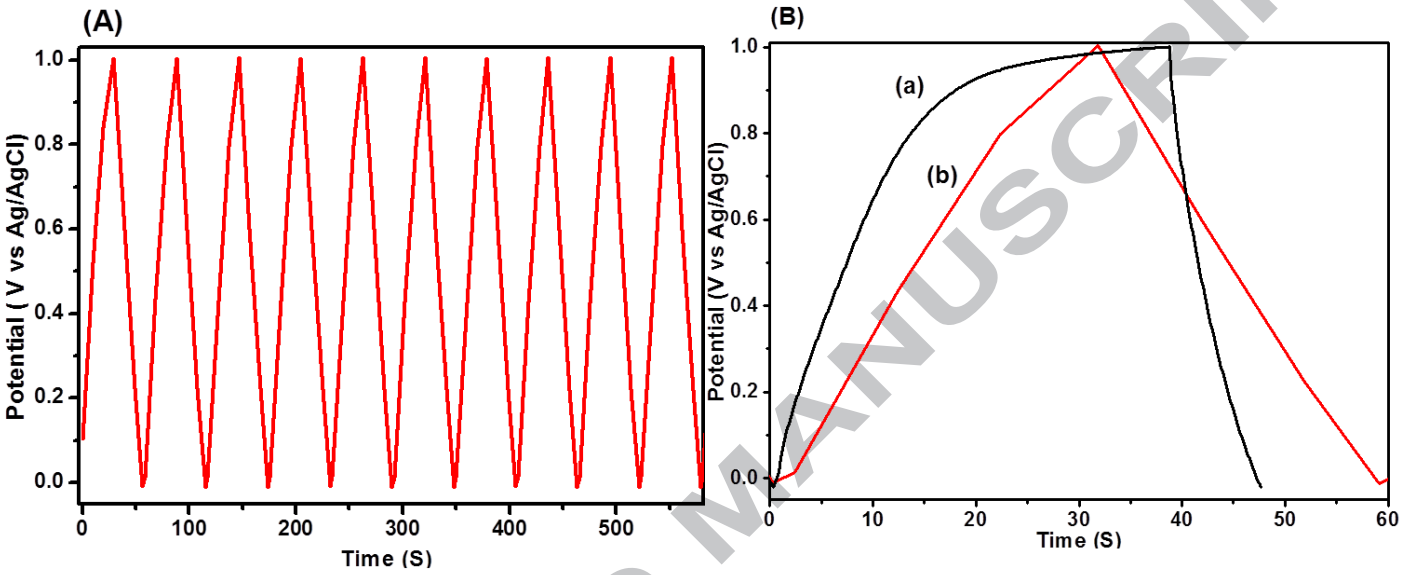

Fig. 8. (A) Galvanostatic Charge–discharge behavior of the prepared SnO_2/MWCNT nanocomposites. Fig. 7(B) Charge/discharge curves of (a) SnO_2/VC and (b) SnO_2/MWCNT in aqueous solution of 1 M Na_2SO_4 at a current density of 0.5mA/cm^2 between 0 and +1 V vs. Ag/AgCl. Area of the electrode: 1 cm^2

Highlights

- Multiwalled carbon nanotubes and Vulcan carbon decorated with SnO_2 nanoparticles were synthesized using a sonochemical procedure
- SnO_2 nanoparticles were uniformly distributed on both the carbon surfaces were identified using TEM analysis
- The electrochemical performance of the nanocomposites was evaluated by cyclic voltammetry and galvanostatic charge/discharge cycling
- SnO_2/MWCNTs electrodes exhibit a specific capacitance of 133.33 Fg^{-1} whereas SnO_2/VC electrodes exhibit only 112.14 Fg^{-1}